

Host–Guest Systems | *Hot Paper* | A New Biscarbazole-Based Metal–Organic Framework for Efficient Host–Guest Energy TransferQianqian Mu,^[a] Jingjuan Liu,^[a] Weiben Chen,^[a] Xiaoyu Song,^[a] Xiaoting Liu,^[b]
Xiaotao Zhang,^{*[a]} Ze Chang,^{*[b]} and Long Chen^{*[a]}

Abstract: A new metal–organic framework (MOF), [Zn₆L₄(Me₂NH₂⁺)₄·3H₂O] (**1**) was constructed based on [9, 9'-biscarbazole]-3, 3', 6, 6'-tetracarboxylic acid (H₄L) and Zn²⁺ ions. The porous framework and intense blue fluorescence of the MOF based on the biscarbazole moiety of the ligand could facilitate efficient host to guest energy transfer, which makes it an ideal platform for the tuning of luminescence.

Metal–organic frameworks (MOFs) are porous crystalline materials constructed by metal ions or metal clusters and organic ligands through coordination bonds.^[1] By varying the metal ions, organic ligands, and/or synthetic conditions, numerous MOFs with different structures and properties can be obtained. Because of their attractive properties, including large surface areas, tunable porosity, and variable structure, MOFs were widely used in the realms of gas storage and separation,^[2] catalysis,^[3] sensing,^[4] drug delivery and bio-imaging,^[5] optoelectronics,^[6] energy storage and conversion,^[7] and so on. In addition to these applications, luminescent MOFs^[8] have been developed as a unique platform for highly efficient energy transfer utilizing their unique pore structure and photophysical properties. For example, Hupp and co-workers reported a quantum dots@porphyrin-based MOFs composites for the enhancement of light harvesting via energy transfer from the quantum dots to the MOFs.^[9] Du et al. have reported a dual-emitting dye@MOF composite showing apparent energy transfer process from MOF to dye.^[10] Our group recently reported a tetraphenylethylene-based luminescent MOF with excellent light-harvesting properties with a host to guest energy transfer efficiency up to 96%.^[11]

In consideration of the mechanism of energy transfer, there are several principles for the construction of energy transfer systems with MOFs. Firstly, to simplify the engineering of ligand-based emission and avoid the emission quenching, transition-metal ions without unpaired electrons is preferred, especially those having d¹⁰ configurations.^[8] Secondly, because the energy transfer process requires a short distance between the donor and acceptor, a highly porous framework with proper pore structure is preferred as the host so that guest molecules could contact with the host framework more effectively. Furthermore, the porous framework could also promote the loading and dispersion of the guest, which could facilitate the energy transfer between the host and guest. For the construction of porous MOF as host, one of the important factors that should be considered is the structure of organic ligand. In the perspective of topology, the connection and configuration of the ligand could determine the structure of the MOF. It has been proved that multidentate carboxylate ligands could promote the formation of highly porous MOFs. For example, several tetra-carboxylate ligands with planar backbones have been well studied, such as tetraphenylethylene,^[11,12] porphyrin,^[13] tetraphenylbenzene,^[14] pyrene,^[15] etc. In contrast, ligands with steric backbones such as 9,9'-spirobifluorene^[16] and tetraphenylmethane^[17] were rarely reported. Among the various potential backbones, *N, N'*-biscarbazole has caught our attention for its steric geometry, which has rarely been utilized for the construction of MOFs. On the other hand, the carbazole has been widely used in the construction of organic luminophores owing to its unique emission properties, which is also desired for the construction of energy transfer platform.

In this work, we designed and synthesized a multidentate ligand, [9, 9'-biscarbazole]-3, 3', 6, 6'-tetracarboxylic acid (H₄L), for the construction of MOF as a platform for energy transfer. Based on this ligand, a three dimensional Zn^{II} porous MOF was synthesized, namely [Zn₆L₄(Me₂NH₂⁺)₄·3H₂O] (**1**). This MOF exhibits a ligand-originated broad emission around 460 nm and a relatively high porosity, indicating its potential as an ideal host for the construction of energy transfer system. On the basis of these characteristics, we further investigated the energy transfer behaviors of the MOF by encapsulating different dye molecules into **1** (e.g., coumarin 6 or rhodamine 6G, Scheme S3). The results show that highly efficient energy transfer could occur between the MOF as host and the dyes as guest, which prove the current MOF to be an ideal platform for energy transfer.

[a] Q. Mu, J. Liu, W. Chen, X. Song, Prof. X. Zhang, Prof. L. Chen
Department of Chemistry, Tianjin Key Laboratory of Molecular Optoelectronic Science and Institute of Molecular Plus, Tianjin University, Tianjin, 300072 (P. R. China)

E-mail: zhangxt@tju.edu.cn
long.chen@tju.edu.cn

[b] X. Liu, Prof. Z. Chang
School of Materials Science and Engineering, National Institute for Advanced Materials, TKL of Metal and Molecular-Based Material Chemistry, Nankai University, Tianjin 300350 (P. R. China)
E-mail: changze@nankai.edu.cn

 Supporting information and the ORCID identification number(s) for the author(s) of this article can be found under:
<https://doi.org/10.1002/chem.201805636>

Colorless block crystals of **1** could be obtained by solvothermal reaction of $\text{Zn}(\text{NO}_3)_2 \cdot 6\text{H}_2\text{O}$ and H_4L in the mixture of *N,N*-dimethylformamide (DMF), 1,4-dioxane, and H_2O (V:V:V = 2:1:1) at 90 °C for four days. Single-crystal X-ray diffraction analysis revealed that MOF **1** crystallizes in monoclinic space group *C2/c* (Table S1, Supporting Information). The asymmetric unit of the MOF contains 1.5 Zn^{II} ions, one L^{4-} ligand and one Me_2NH_2^+ counter ion (Figure 1). Other free solvent molecules were diffi-

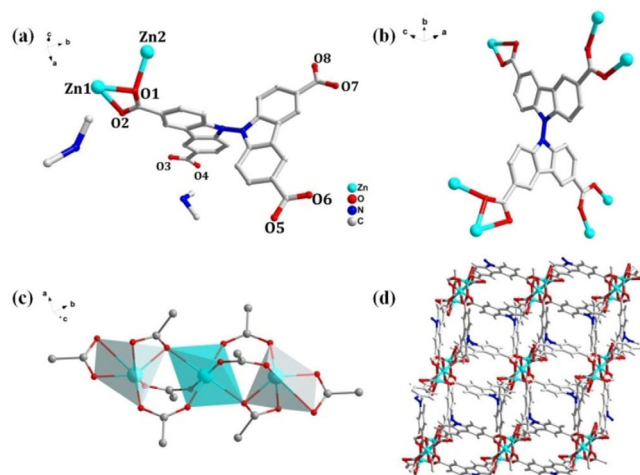


Figure 1. The structure of **1**: (a) asymmetric unit; (b) coordination mode of the L^{4-} ligand; (c) $[\text{Zn}_3(\text{CO}_2)_8]$ trinuclear clusters; (d) the 3D framework structure of **1**.

cult to be modulated because of their highly disordered state. The L^{4-} ligand reveals $\mu_7-(\eta_1-\eta_1-\mu_1)-(\eta_1-\eta_2-\mu_2)-(\eta_1-\eta_1-\mu_2)-(\eta_1-\eta_1-\mu_2)$ coordination mode to bridge seven Zn^{II} ions. Zn1 reveals a distorted octahedral coordination geometry defined by six carboxyl oxygen atoms from four ligands. For Zn2, it is surrounded by six oxygen atoms from five L^{4-} ligands to give another distorted octahedral coordination geometry. Zn1 and Zn2 metal centers were bridged through two bidentate and one tridentate bridging carboxylate groups from three L^{4-} ligands, and the neighboring three Zn^{II} atoms interconnect with each other to form a $[\text{Zn}_3(\text{CO}_2)_8]$ trinuclear cluster as secondary building unit (SBU).

Each $[\text{Zn}_3(\text{CO}_2)_8]$ cluster connects with eight L^{4-} ligands, and each L^{4-} ligand links to four $[\text{Zn}_3(\text{CO}_2)_8]$ clusters. The connection between the ligands and the clusters generate a three-dimensional (3D) porous framework with square 1D channels along the *a*-axis ($\sim 13.6 \times 15.7 \text{ \AA}^2$), which are occupied by free Me_2NH_2^+ counter ions and free solvent molecules. After removal of solvent molecules, the accessible volume of **1** is 49% (1267.7 \AA^3 of the 3720 \AA^3 unit cell volume), as estimated using the SQUEEZE routine in PLATON.^[18]

The phase purity of **1** was verified by powder X-ray diffraction (PXRD) measurements. As shown in Figure S5, the PXRD pattern of the as-synthesized **1** matches well with the simulated patterns based on the crystal structure, indicating the high phase purity of bulk sample. The thermogravimetric analysis (TGA) results reveal that the framework is thermally stable up

to ca. 320 °C. The N_2 sorption isotherm for **1** recorded at 77 K exhibits a characteristic type-I profile, which reveals the microporous nature of **1** (Figure S7). The BET surface area of the sample was determined to be $789 \text{ m}^2 \text{ g}^{-1}$, and the pore size distribution analysis of **1** indicate that the accessible pore dimension is about 9 Å (Figure S8). All these results suggest that **1** could serve as a host for the loading of guest molecules.

In consideration of the carbazole backbone that commonly exhibits intense deep-blue emissions, **1** is expected to show similar emissions that could facilitate its application as donor host for energy transfer. Therefore, the luminescence of the H_4L ligand and **1** were investigated in solid state at room temperature. Both of them exhibits intense blue luminescence upon the excitation of UV light. As shown in Figure S10, H_4L ligand exhibits a broad emission band around 440 nm when excited at 380 nm. Similarly, MOF **1** displays a broad emission band at 460 nm, which could be assigned to the emission from the ligand considering the similar wavelength and band shape. The slight redshift (20 nm) might be due to the change of the configuration of the ligand upon coordination to the metal ions.^[19] The intense and broad emission of **1** suggest its potential as donor for energy transfer, since highly efficient energy transfer could be achieved with various acceptors with different excitations.

To further investigate the potential of **1** as platform for energy transfer applications, energy transfer system was fabricated with **1** as host and fluorescent dye as guest. As one of the typical red emissive dyes, Rh6G was selected in consideration of its proper dimension and excitation. As shown in Figure 3a (see below), the distinctive color change upon in situ incorporation of Rh6G indicates the successful loading of Rh6G into **1**, which is named as Rh6G@**1**. The PXRD patterns of Rh6G@**1** composites matched well with that of **1**, which indicates that the framework structure of **1** is well retained after introduction of dye molecules (Figure S11). Furthermore, there was no leakage of Rh6G guest from the Rh6G@**1** after the sample soaked in DMF for 24 h, which was confirmed by the UV/Vis spectra of the supernatant (Figure S12). This result suggest that the dye molecules could be well encapsulated in the host framework of **1**, which should be ascribed to the well matched pore size of **1** (ca. 9 Å) to the molecular size of the Rh6G ($10.89 \times 15.72 \times 15.79 \text{ \AA}^3$).^[10]

As shown in Figure 2, the emission spectra of Rh6G in DMF ($2 \times 10^{-5} \text{ mol L}^{-1}$) exhibits a maximal peak at 567 nm with excitation at 513 nm. The overlap between the emission of **1** and the excitation spectra of Rh6G suggests the potential of efficient energy transfer from **1** to Rh6G. Solid-state fluorescence spectra of Rh6G@**1** further confirmed the energy transfer process. As displayed in Figure 3b, the fluorescence spectra of Rh6G@**1** presents two emission bands at 450 and 565 nm when irradiated at 380 nm, which are originated from the MOF host and guest Rh6G molecules, respectively. With the increase loading of Rh6G, the emission intensity of **1** gradually decreased, whereas the emission of Rh6G increased. Meanwhile, the emission color of the corresponding samples changed from blue to orange (Figure 3a). These results suggest the occurrence of energy transfer from **1** to Rh6G guests. Meanwhile,

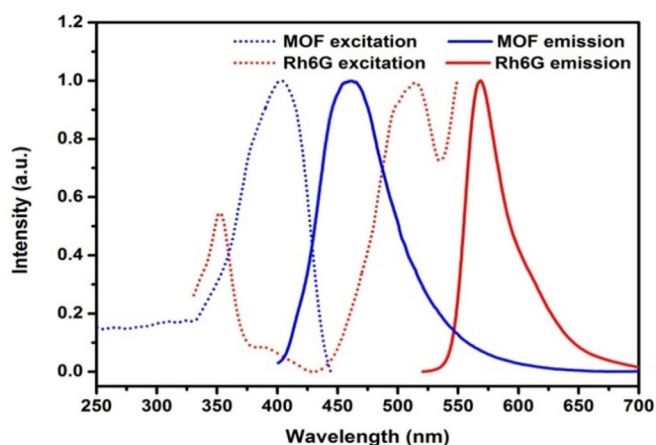


Figure 2. Fluorescence excitation (dotted) and emission (solid) spectra of **1** (dotted blue curve monitored at 465 nm, solid blue curve upon excitation at 380 nm) and Rh6G (dotted red curve monitored at 567 nm, solid red curve upon excitation at 500 nm, in DMF solution).

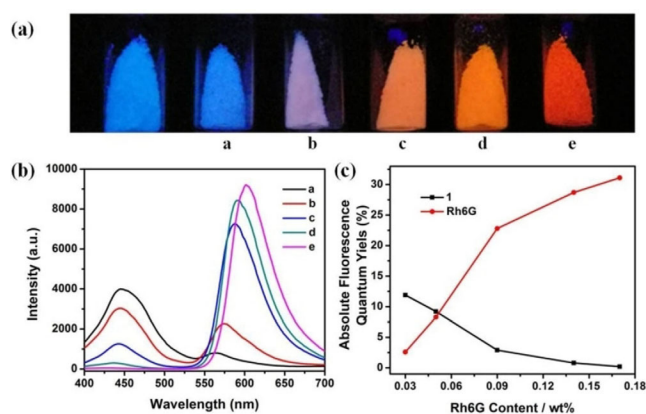


Figure 3. (a) Fluorescence photographs of solid samples of **1** and Rh6G@**1** with different loadings of Rh6G upon excited at 365 nm; (b) The fluorescence emission spectra for Rh6G@**1** upon excitation at 380 nm (a = 0.03 wt%, b = 0.05 wt%, c = 0.09 wt%, d = 0.14 wt%, e = 0.17 wt%); (c) the absolute fluorescence quantum yield (Φ_f) of **1** and Rh6G under excitation at 380 nm.

we compared the emission spectra of Rh6G@**1**-e and that of thoroughly ground mixture of Rh6G and **1** (Rh6G = 0.17 wt%) measured under the same conditions. The emission spectra of the mechanically ground mixture only exhibits a broad emission at about 460 nm, which is originated from **1** (Figure S13). These results clearly indicate the absence of energy transfer in the mechanical mixed sample, since the particles of MOF and dye could not contact well to meet the distance required for energy transfer with this method. Furthermore, the absence of emission of dye in this sample should be due to the aggregation induced quenching in solid state, which accord well with the weak emission of Rh6G in solid state (Figure S14). Then the enhanced emission of Rh6G in the MOF may benefit from the highly dispersion of dye molecules in the host framework of **1** through the avoid of aggregation-caused quenching.^[20]

Furthermore, for the quantitative proof of the host to dye energy transfer process, the fluorescence quantum yield (Φ_f)

of Rh6G@**1** were determined. As shown in Figure 3 c, the Φ_f of **1** decreased from 11.9 to 0.1%, whereas the Φ_f of Rh6G increased from 2.6 to 30.1% with increasing Rh6G loading. The results proved that the light energy transferred from MOF host to the guest dye molecules, and the energy transfer efficiency (η_{ET}) estimated from the quenching rate of MOF emission ($\eta_{ET} = 1 - \Phi_f(c)/\Phi_f(0)$,^[21] where c is Rh6G concentration) reaches 98.8% (Table S4). Thus, our example represents one of the most efficient host-guest energy transfer in light-harvesting MOF systems (Table S9). Furthermore, we measured the lifetime of the emission of host framework to evaluate the rate constant of the energy transfer. The average lifetime of **1** (τ_0) was measured to be 7.63 ns (Figure 4, black curve). For the

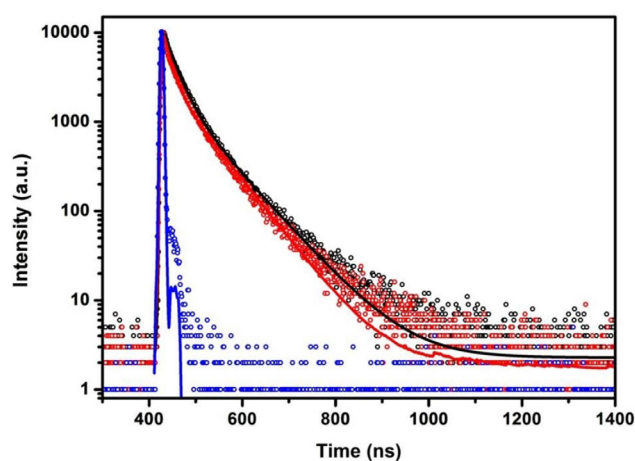


Figure 4. Fluorescence decay profiles of pristine **1** (black dots) monitored at 460 nm and the host in Rh6G@**1** samples (a, red dots monitored at 455 nm and e, blue dots monitored at 430 nm), the solid lines represent the best-fit using a global multiexponential function.

Rh6G@**1**, the average lifetime of MOF host (τ_{DA}) changed from 6.18 to 0.16 ns with increasing Rh6G content (Figure 4, red and blue curve). Accordingly, the rate constant of energy transfer ($k_{ET} = \tau_{DA}^{-1} - \tau_0^{-1}$)^[22] from MOF **1** to Rh6G increased from 0.03×10^9 to $6.12 \times 10^9 \text{ s}^{-1}$ (Table S5). Both the high η_{ET} and k_{ET} values suggest the high efficiency of the energy transfer process. This excellent energy transfer performance should be ascribed to the highly porous framework of **1**. Because the dye molecules could be encapsulated well in the framework of **1**, a close contact could be expected between the host and the guests. In consideration of the FRET mechanism of energy transfer, the short distance between the donor and the acceptor would benefits the energy transfer process.

Furthermore, owing to the broad emission band and considerable porous framework of **1**, we expected that dye molecules with distinct emissions could be introduced aiming at the targeted construction of luminophores. As a representative coumarin derivative, coumarin 6 (C6) is a typical green emissive fluorescent dye. Since the emission spectra of **1** and the adsorption spectra of C6 are overlapped well, the C6@**1** could be expected to be an ideal green luminophore on the basis of the effective energy transfer in this system (Figure S15b). C6@**1**

was obtained through a similar in situ synthesis procedure with that of Rh6G@1. The emission color of sample changed from blue to green after encapsulation of C6 molecules (Figure S15a). This phenomenon initially indicates that the dye molecules have been successfully loaded into 1. As shown in Figure S15c, the fluorescence spectra of C6@1 also exhibits two emission band at about 440 and 500 nm, which are originated from 1 and C6, respectively. The emission of MOF host receded while the green emission of C6 enhanced with the increase of the loading content of C6, similar to the result of Rh6G@1, indicating the occurrence of energy transfer between the host and the C6 guests. Similarly, we measured the quantum yields of C6@1 with different dye loading (a–e) (Figure S15d). The Φ_{fl} of 1 decreased from 2.8 to 0.8%, whereas the Φ_{fl} of C6 increased from 3.4 to 11.0%. The changes of quantum yields verified the energy transfer process. The energy transfer efficiency (η_{ET}) estimated from the quenching rate of MOF emission ($\eta_{ET} = 1 - \Phi_{fl}(c)/\Phi_{fl}(0)$, where c is C6 concentration) reaches 95.0%. The lifetime (τ_{DA}) of C6@1 decreased from 1.43 to 0.36 ns with the increase of C6 loading (Figure S15e), and the rate constant increased from 0.57×10^9 to $2.64 \times 10^9 \text{ s}^{-1}$ accordingly. All of these results confirmed the efficient energy transfer from the MOF host to the guest dye molecules. All these results indicate that C6@1 is also a highly efficient energy transfer system, and the MOF 1 is an ideal energy transfer platform.

In conclusion, through the application of a new tetracarboxylate ligand with spatially vertical 9, 9'-bicarbazole backbone, a new Zn^{II} MOF with intense blue luminescence and permanent porosity was synthesized, which could serve as an energy transfer platform. By encapsulating different fluorescence dyes into the MOF, a series of dual-emitting dye@MOF composites were obtained. The photophysical properties of dye@MOF composites indicate that efficient energy transfer could occur between the host and the guests, with an efficiency (η_{ET}) up to 98.8%. Beyond the successful construction of a new energy transfer platform, our achievement herein also provides a new platform for targeted construction of luminophores.

Experimental Section

Experimental and synthesis procedures; crystallographic data; NMR, FT-IR, UV/Vis, and fluorescence spectra; TGA profile, PXRD patterns, nitrogen sorption isotherm, pore size distribution; and photoluminescence properties can be found in the Supporting Information.

Acknowledgements

This work was supported by the National Natural Science Foundation of China (51522303, 21602154), the National Key Research and Development Program of China (2017YFA0207500), and the Natural Science Foundation of Tianjin (17JJCJC44600).

Conflict of interest

The authors declare no conflict of interest.

Keywords: energy transfer • fluorescence • host–guest systems • in situ encapsulation • metal–organic frameworks

- [1] a) H. Furukawa, N. Ko, Y. B. Go, N. Aratani, S. B. Choi, E. Choi, A. Ö. Yazaydin, R. Q. Snurr, M. O'Keeffe, J. Kim, O. M. Yaghi, *Science* **2010**, *329*, 424; b) Y. Cui, B. Li, H. He, W. Zhou, B. Chen, G. Qian, *Acc. Chem. Res.* **2016**, *49*, 483–493; c) M. Eddaoudi, D. F. Sava, J. F. Eubank, K. Adil, V. Guillerm, *Chem. Soc. Rev.* **2015**, *44*, 228–249; d) P. Silva, S. M. F. Vilela, J. P. C. Tome, F. A. Almeida Paz, *Chem. Soc. Rev.* **2015**, *44*, 6774–6803; e) H.-C. Zhou, J. R. Long, O. M. Yaghi, *Chem. Rev.* **2012**, *112*, 673–674.
- [2] a) J.-R. Li, R. J. Kuppler, H.-C. Zhou, *Chem. Soc. Rev.* **2009**, *38*, 1477–1504; b) A. R. Millward, O. M. Yaghi, *J. Am. Chem. Soc.* **2005**, *127*, 17998–17999; c) Y. Yan, M. Juriček, F.-X. Coudert, N. A. Vermeulen, S. Grunder, A. Dailly, W. Lewis, A. J. Blake, J. F. Stoddart, M. Schröder, *J. Am. Chem. Soc.* **2016**, *138*, 3371–3381.
- [3] a) J. S. Seo, D. Whang, H. Lee, S. I. Jun, J. Oh, Y. J. Jeon, K. Kim, *Nature* **2000**, *404*, 982; b) J. Lee, O. K. Farha, J. Roberts, K. A. Scheidt, S. T. Nguyen, J. T. Hupp, *Chem. Soc. Rev.* **2009**, *38*, 1450–1459; c) H. Mao, W. Zhang, W. Zhou, B. Zou, B. Zheng, S. Zhao, F. Huo, *ACS Appl. Mater. Interfaces* **2017**, *9*, 24649–24654.
- [4] a) M. Zheng, H. Tan, Z. Xie, L. Zhang, X. Jing, Z. Sun, *ACS Appl. Mater. Interfaces* **2013**, *5*, 1078–1083; b) X.-L. Yang, X. Chen, G.-H. Hou, R.-F. Guan, R. Shao, M.-H. Xie, *Adv. Funct. Mater.* **2016**, *26*, 393–398; c) X. Zhao, Y. Li, Z. Chang, L. Chen, X.-H. Bu, *Dalton Trans.* **2016**, *45*, 14888–14892.
- [5] P. Horcajada, R. Gref, T. Baati, P. K. Allan, G. Maurin, P. Couvreur, G. Férey, R. E. Morris, C. Serre, *Chem. Rev.* **2012**, *112*, 1232–1268.
- [6] a) C. Wang, T. Zhang, W. Lin, *Chem. Rev.* **2012**, *112*, 1084–1104; b) D. F. Sava, L. E. S. Rohwer, M. A. Rodriguez, T. M. Nenoff, *J. Am. Chem. Soc.* **2012**, *134*, 3983–3986.
- [7] a) A. Morozan, F. Jaouen, *Energy Environ. Sci.* **2012**, *5*, 9269–9290; b) T. C. Narayan, T. Miyakai, S. Seki, M. Dincă, *J. Am. Chem. Soc.* **2012**, *134*, 12932–12935; c) L. Sun, T. Miyakai, S. Seki, M. Dincă, *J. Am. Chem. Soc.* **2013**, *135*, 8185–8188.
- [8] Z. Hu, B. J. Deibert, J. Li, *Chem. Soc. Rev.* **2014**, *43*, 5815–5840.
- [9] S. Jin, H.-J. Son, O. K. Farha, G. P. Wiederrecht, J. T. Hupp, *J. Am. Chem. Soc.* **2013**, *135*, 955–958.
- [10] D.-M. Chen, N.-N. Zhang, C.-S. Liu, M. Du, *ACS Appl. Mater. Interfaces* **2017**, *9*, 24671–24677.
- [11] X. Zhao, X. Song, Y. Li, Z. Chang, L. Chen, *ACS Appl. Mater. Interfaces* **2018**, *10*, 5633–5640.
- [12] N. B. Shustova, B. D. McCarthy, M. Dincă, *J. Am. Chem. Soc.* **2011**, *133*, 20126–20129.
- [13] a) X.-S. Wang, M. Chrzanowski, W.-Y. Gao, L. Wojtas, Y.-S. Chen, M. J. Zaworotko, S. Ma, *Chem. Sci.* **2012**, *3*, 2823–2827; b) X.-S. Wang, M. Chrzanowski, C. Kim, W.-Y. Gao, L. Wojtas, Y.-S. Chen, X. Peter Zhang, S. Ma, *Chem. Commun.* **2012**, *48*, 7173–7175.
- [14] a) C. Y. Lee, Y.-S. Bae, N. C. Jeong, O. K. Farha, A. A. Sarjeant, C. L. Stern, P. Nickias, R. Q. Snurr, J. T. Hupp, S. T. Nguyen, *J. Am. Chem. Soc.* **2011**, *133*, 5228–5231; b) K. L. Mulfort, O. K. Farha, C. D. Malliakas, M. G. Kanatzidis, J. T. Hupp, *Chem. Eur. J.* **2010**, *16*, 276–281.
- [15] a) R.-J. Li, M. Li, X.-P. Zhou, D. Li, M. O'Keeffe, *Chem. Commun.* **2014**, *50*, 4047–4049; b) Y.-L. Huang, Y.-N. Gong, L. Jiang, T.-B. Lu, *Chem. Commun.* **2013**, *49*, 1753–1755.
- [16] P. K. Clews, R. E. Douthwaite, B. M. Kariuki, T. Moore, M. Taboada, *Cryst. Growth Des.* **2006**, *6*, 1991–1994.
- [17] a) M. Almasi, V. Zelenak, A. Zukal, J. Kuchar, J. Cejka, *Dalton Trans.* **2016**, *45*, 1233–1242; b) H. Furukawa, F. Gándara, Y.-B. Zhang, J. Jiang, W. L. Queen, M. R. Hudson, O. M. Yaghi, *J. Am. Chem. Soc.* **2014**, *136*, 4369–4381.
- [18] A. L. Spek, *J. Appl. Crystallogr.* **2003**, *36*, 7.
- [19] Z. Wei, Z.-Y. Gu, R. K. Arvapally, Y.-P. Chen, R. N. McDougald, J. F. Ivy, A. A. Yakovenko, D. Feng, M. A. Omary, H.-C. Zhou, *J. Am. Chem. Soc.* **2014**, *136*, 8269–8276.

- [20] a) R. H. Friend, R. W. Gymer, A. B. Holmes, J. H. Burroughes, R. N. Marks, C. Taliani, D. D. C. Bradley, D. A. D. Santos, J. L. Brédas, M. Lögdlund, W. R. Salaneck, *Nature* **1999**, *397*, 121; b) Z. Yuan Wang, P. Lu, S. Chen, W. Y. Lam Jacky, Z. Wang, Y. Liu, S. Kwok Hoi, Y. Ma, Z. Tang Ben, *Adv. Mater.* **2010**, *22*, 2159–2163.
- [21] S. Inagaki, O. Ohtani, Y. Goto, K. Okamoto, M. Ikai, K. Yamanaka, T. Tani, T. Okada, *Angew. Chem. Int. Ed.* **2009**, *48*, 4042–4046; *Angew. Chem.* **2009**, *121*, 4102–4106.
- [22] C. Gu, N. Huang, F. Xu, J. Gao, D. Jiang, *Sci. Rep.* **2015**, *5*, 8867.

Manuscript received: November 12, 2018
Revised manuscript received: December 10, 2018
Version of record online: ■ ■ ■ ■, 0000

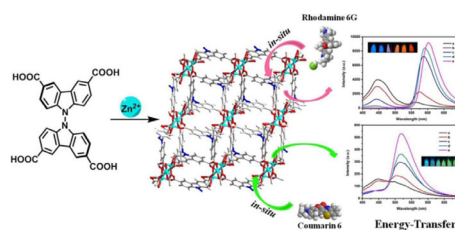
COMMUNICATION

Host–Guest Systems

Q. Mu, J. Liu, W. Chen, X. Song, X. Liu,
X. Zhang,* Z. Chang,* L. Chen*



A New Biscarbazole-Based Metal–Organic Framework for Efficient Host–Guest Energy Transfer



When the MOFs go blue: A metal organic framework (MOF) was constructed based on a novel biscarbazole tetracar-

boxylic acid ligand. This blue fluorescent MOF serves as an ideal platform for host–guest energy transfer.